

TURBULENT HEAT TRANSFER IN A BACK-STEP FLOW PAST A POROUS OBSTRUCTION USING A NON-LINEAR MODEL AND A LOW REYNOLDS NUMBER FORMULATION

Marcelo Assato

Marcelo J.S. De-Lemos*

Departamento de Energia – IEME

Instituto Tecnológico de Aeronáutica – ITA

12228-900 - São José dos Campos - SP – Brazil

* Corresponding author, e-mail: delemos@mec.ita.br

Abstract. This paper presents a numerical investigation of turbulent flow past a backward-facing-step channel with a porous obstruction using linear and nonlinear $k - \epsilon$ macroscopic models. Results were obtained considering an inlet Reynolds number of $Re = 132000$ based on the height of the step. In clean medium, the literature has shown a better prediction using the nonlinear model in turbulent flows that present accentuated curvatures in their streamlines. The present case involves a hybrid medium and parameters such as porosity, permeability and thickness of the porous obstruction are varied in order to analyze their effects on the flow pattern, particularly on the damping of the re-circulating bubble after the porous insertion. Equations are discretized using the control-volume method applied to a boundary-fitted coordinate system with a collocated grid. The SIMPLE algorithm was used to relax the algebraic equations. Low Reynolds damping functions are employed for handling wall proximity. Comparisons of results simulated with both linear and nonlinear turbulence models are shown.

Keywords. porous obstruction, turbulent heat transfer, non-linear model, low Reynolds number

1. Introduction

Flows presenting separation and reattachment have been the subject of various research efforts during the last decades. Such flows occur in gas turbine, nuclear reactors, and heat transfer devices, for example. The recirculating zone close to heated wall causes large variations in the local heat transfer coefficient, ultimately leading to overall heat transfer augmentation around the reattachment point. Thus, sometimes the attenuation or even the suppression of the recirculating bubble is desired. The placement of a material (such as, honeycombs or screens) inside a fluid passageway can attenuate recirculation zones and produce a uniform flow with low turbulence. Depending on certain parameter, such as insert thickness, porosity and directional permeability, such components may be treated as a porous medium positioned within the flow. In addition, many engineering problems have flows involving interfaces between a porous medium and a clear medium. The problem of boundary conditions at the porous medium/clear fluid interface has been dealt by several authors [Beavers and Joseph (1967), Vafai and Tien (1981), Vafai and Kim (1990), Ochoa-Tapia and Whitaker (1995)].

More specifically, the problem of flow past a backward-facing step with porous inserts has been study by Rocamora and de Lemos (2000) and Chan et al. (2000). Both works presented laminar and turbulent results with forced convective heat transfer. They used for modeling turbulent flow a two-equation linear $k - \epsilon$ model with wall function for both the fluid region and the porous medium. Rocamora and de Lemos (2000) treat the interface between the porous medium and the clear fluid following the work in Ochoa-Tapia and Whitaker (1995). Chan et al. (2000) considered the flow at the interface between the fluid and porous medium as being continuous. The presence of the Brinkman's extension model [Brinkman (1948)] in the porous media equation eliminates the need for imposing an explicit interface condition, in accordance with Nield and Bejan (1992). More recently, Assato et al. (2002) simulated the case of flow past a backward-facing step with porous obstruction, however without heat transfer. They using the turbulence $k - \epsilon$ linear and non-linear models with wall function.

In this work, numerical results for heat transfer in turbulent flow past a backward-facing step in a channel with a porous obstruction are presented. Low number Reynolds damping functions for the velocity field are used in conjunction with both *linear* and *non-linear* eddy viscosity macroscopic models to describe the flow near the walls. Here, the boundary conditions at the porous medium/clear fluid interface are the same used by Rocamora and de Lemos (2000) and Assato et al. (2002).

In the literature, the linear $k - \epsilon$ model, in combination with the assumption of a constant turbulent Prandtl number, has been often used to predict heat transfer in separating and reattaching flows. However, a literature survey reveals that the standard $k - \epsilon$ model under-predicts the reattachment point location by an amount on the order of 20-25%. In fact, it is well established in the literature that the linear $k - \epsilon$ model do not, on the whole, cope well with strong streamline curvature whether it arises from flow over curved surfaces or imparted swirling. And yet, turbulence-driven secondary motion and directional effects due to buoyancy cannot, due to absence of information on individual stresses, be fully simulated with the standard $k - \epsilon$ model. In spite of that, it is frequently used for engineering computations due to the numerical robustness obtained via its linear stress-strain rate relationship (Jones and Launder (1972)).

Non-linear models represent an extension of the standard two-equation closure and have shown good performance in flows with recirculation and where normal stresses play an important role (Assato & de Lemos (2000)). Basically, they follow the procedures used in obtaining constitutive equations for laminar flow of non-Newtonian fluids (Rivlin

(1957)). Example is the work of Speziale (1987). Essentially, the observed relationship between laminar flow of viscoelastic fluids and turbulent flow of Newtonian substances has motivated developments of such Non-Linear Models (Lumley (1970)). Other works on this subject are of Nisizima and Yoshizawa (1987), Rubinstein & Barton (1990) and Shih et al (1993). In those papers, quadratic products were introduced involving the strain and vorticity tensors with different derivations and calibrations for each model. The basic advantage of these non-linear techniques over more complex closures, such as the Algebraic Stress Models (e.g. de Lemos & Sesonke (1985), de Lemos (1988)) lies on the achieved computational savings (roughly 25-50% less computing time).

Therefore, in this article comparisons of results simulated with both linear and non-linear $k-\varepsilon$ turbulence models and a low Reynolds number formulation for heat transfer in turbulent flow past a backward-facing step in a channel with a porous obstruction are shown. Some important parameters such as porosity, permeability and thickness of the porous obstruction are varied and their effects on the flow are assessed.

2. Macroscopic transport and constitutive equations

The development presented in References [Pedras and de Lemos (2001a), (2001b), (2001c), (2002)] assumes single-phase flow in a saturated, rigid porous medium (ΔV_f independent of time), for which time-average operation on variable commutes with space average. For this situation, Pedras and de Lemos (2001a) present the following macroscopic equations system:

Macroscopic continuity equation:

$$\nabla \cdot \bar{\mathbf{u}}_D = 0, \quad (1)$$

where, $\bar{\mathbf{u}}_D$ is the average surface velocity ('seepage' or Darcy velocity). The equation (1) represents the macroscopic continuity equation for an incompressible fluid.

Macroscopic momentum equation:

$$\left[\nabla \cdot \left(\rho \frac{\bar{\mathbf{u}}_D \bar{\mathbf{u}}_D}{\phi} \right) \right] = -\nabla(\phi \langle \bar{p} \rangle^i) + \mu \nabla^2 \bar{\mathbf{u}}_D + \nabla \cdot (-\rho \phi \langle \overline{\mathbf{u}' \mathbf{u}'} \rangle^i) - \left[\frac{\mu \phi}{K} \bar{\mathbf{u}}_D + \frac{c_F \phi \rho |\bar{\mathbf{u}}_D| \bar{\mathbf{u}}_D}{\sqrt{K}} \right], \quad (2)$$

where the last two terms in equation (2), represent the Darcy-Forchheimer contribution. The symbol K is the porous medium permeability, c_F is the form drag coefficient (Forchheimer coefficient), $\langle \bar{p} \rangle^i$ is the intrinsic average pressure of the fluid, ρ is the fluid density, μ represents the fluid viscosity and ϕ is the porosity of the porous medium. The macroscopic Reynolds stress $-\rho \phi \langle \overline{\mathbf{u}' \mathbf{u}'} \rangle^i$ is given below.

Macroscopic Reynolds Stress:

A macroscopic linear stress-strain rate relationship was given by Pedras and de Lemos (2001a) as,

$$-\rho \phi \langle \overline{\mathbf{u}' \mathbf{u}'} \rangle^i = \mu_{t_\phi} \langle \bar{\mathbf{D}} \rangle^v - \frac{2}{3} \phi \rho \langle k \rangle^i \mathbf{I}, \quad (3)$$

in analogy with clear flow cases. In (3) the term,

$$\langle \bar{\mathbf{D}} \rangle^v = \left[\nabla \bar{\mathbf{u}}_D + [\nabla \bar{\mathbf{u}}_D]^T \right], \quad (4)$$

represents the mean deformation tensor and \mathbf{I} is the unity tensor.

Macroscopic eddy viscosity:

$$\mu_{t_\phi} = \rho c_\mu f_\mu \frac{\langle k \rangle^i}{\langle \varepsilon \rangle^i}, \quad (5)$$

where $c_\mu = 0.09$ and $\langle k \rangle^i$ and $\langle \varepsilon \rangle^i$ are the intrinsic averages of the turbulent kinetic energy and its dissipation rate, respectively and f_μ is a damping function.

Macroscopic turbulent kinetic energy equation:

$$\rho \nabla \cdot (\bar{\mathbf{u}}_D \langle k \rangle^i) = \nabla \cdot \left[\left(\mu + \frac{\mu_{t_\phi}}{\sigma_k} \right) \nabla (\phi \langle k \rangle^i) \right] - \rho \langle \overline{\mathbf{u}' \mathbf{u}'} \rangle^i : \nabla \bar{\mathbf{u}}_D + c_k \rho \frac{\phi \langle k \rangle^i |\bar{\mathbf{u}}_D|}{\sqrt{K}} - \rho \phi \langle \varepsilon \rangle^i, \quad (6)$$

where $-\rho \langle \overline{\mathbf{u}' \mathbf{u}'} \rangle^i$ is defined by equation (3).

Macroscopic dissipation rate of turbulent kinetic energy equation:

$$\rho \nabla \cdot (\bar{\mathbf{u}}_D \langle \varepsilon \rangle^i) = \nabla \cdot \left[\left(\mu + \frac{\mu_{t_\phi}}{\sigma_\varepsilon} \right) \nabla (\phi \langle \varepsilon \rangle^i) \right] + c_{1\varepsilon} (-\rho \langle \overline{\mathbf{u}' \mathbf{u}'} \rangle^i : \nabla \bar{\mathbf{u}}_D) \frac{\langle \varepsilon \rangle^i}{\langle k \rangle^i} + c_{2\varepsilon} c_k \rho \frac{\phi \varepsilon_\phi |\bar{\mathbf{u}}_D|}{\sqrt{K}} - c_{2\varepsilon} f_\varepsilon \rho \phi \frac{\langle \varepsilon \rangle^i}{\langle k \rangle^i}, \quad (7)$$

where c_k assumes a value equal to 0.28 found by Pedras and de Lemos (2001b), (2001c), (2002). Other constants are defined following the low Reynolds number model of Abe et al (1992).

Macroscopic energy equation:

$$\nabla \cdot \left(\rho \bar{\mathbf{u}}_D T - \frac{k_{eff}}{c_{pf}} \nabla T \right) = s_T, \quad (8)$$

where k_{eff} is the effective thermal conductivity of the saturated porous medium, c_{pf} is the specific heat of the fluid and T represents the average temperature.

It is worthwhile to mention that the surface volume average quantities are related to the intrinsic average quantities through the porosity ϕ as:

$$\langle \phi \rangle^v = \phi \langle \phi \rangle^i. \quad (9)$$

Also, the equations given above are valid for the clear medium as well, setting $\phi=1$ ($K \rightarrow \infty$) and discarding the last two terms in equation (2).

Macroscopic non linear model:

In this work, results produced by non-linear eddy-viscosity models (NLEVM) are investigated. The macroscopic non-linear turbulence model here proposed is constituted by the same system of equations (1)-(7) formerly given by Pedras and de Lemos (2001a). The sole difference between both macroscopic models (Linear and Non-Linear) lies in the expression for the macroscopic Reynolds Stress. Using indexed notation now for clarity and keeping terms to second order, this new macroscopic non-linear stress-strain-rate equation can be rewritten in the form:

$$\begin{aligned} -\rho \phi \langle \overline{\mathbf{u}' \mathbf{u}'} \rangle^i &= \left(\mu_{t_\phi} \langle \bar{D}_{ij} \rangle^v \right)^L - \left(c_{1NL} \mu_{t_\phi} \frac{\langle k \rangle^i}{\langle \varepsilon \rangle^i} \left[\langle \bar{D}_{ik} \rangle^v \langle \bar{D}_{kj} \rangle^v - \frac{1}{3} \langle \bar{D}_{kl} \rangle^v \langle \bar{D}_{kl} \rangle^v \delta_{ij} \right] \right)^{NL1} \\ &\quad - \left(c_{2NL} \mu_{t_\phi} \frac{\langle k \rangle^i}{\langle \varepsilon \rangle^i} \left[\langle \bar{Q}_{ik} \rangle^v \langle \bar{S}_{kj} \rangle^v + \langle \bar{Q}_{jk} \rangle^v \langle \bar{S}_{ki} \rangle^v \right] \right)^{NL2}, \quad (10) \\ &\quad - \left(c_{3NL} \mu_{t_\phi} \frac{\langle k \rangle^i}{\langle \varepsilon \rangle^i} \left[\langle \bar{Q}_{ik} \rangle^v \langle \bar{Q}_{jk} \rangle^v - \frac{1}{3} \langle \bar{Q}_{lk} \rangle^v \langle \bar{Q}_{lk} \rangle^v \delta_{ij} \right] \right)^{NL3} - \frac{2}{3} \phi \delta_{ij} \rho \langle k \rangle \end{aligned}$$

where δ_{ij} is the Kronecker delta; the superscripts (L and NL) in the equation (10) indicate Linear and Non-Linear contributions, μ_{t_ϕ} is again the macroscopic turbulent viscosity given by equation (5), $\langle \bar{D}_{ij} \rangle^v$ and $\langle \bar{Q}_{ij} \rangle^v$ are the deformation and vorticity tensors, written in the indexed form, respectively, as:

$$\langle \bar{D}_{ij} \rangle^v = \left(\frac{\partial \bar{u}_{iD}}{\partial x_j} + \frac{\partial \bar{u}_{jD}}{\partial x_i} \right), \quad \langle \bar{Q}_{ij} \rangle^v = \left(\frac{\partial \bar{u}_{iD}}{\partial x_j} - \frac{\partial \bar{u}_{jD}}{\partial x_i} \right). \quad (11)$$

In this work the non-linear model proposed by Shih et al (1993) was used and has the following expressions:

$$c_\mu = \frac{2/3}{1.25 + s + 0.9\Omega}, \quad c_{1NL} = \frac{0.75}{c_\mu (1000 + s^3)}, \quad c_{2NL} = \frac{3.8}{c_\mu (1000 + s^3)}, \quad c_{3NL} = \frac{4.8}{c_\mu (1000 + s^3)},$$

$$\text{where, } s = \frac{\langle k \rangle^i}{\langle \varepsilon \rangle^i} \sqrt{\frac{1}{2} \langle \overline{D_{ij}} \rangle^v \langle \overline{D_{ij}} \rangle^v} \quad \text{and} \quad \Omega = \frac{\langle k \rangle^i}{\langle \varepsilon \rangle^i} \sqrt{\frac{1}{2} \langle \overline{\Omega_{ij}} \rangle^v \langle \overline{\Omega_{ij}} \rangle^v} \quad (12)$$

Note that equation (3) is recovered if constants c_{1NL} , c_{2NL} and c_{3NL} in (10) are set to zero.

The low Re k- ε model:

The damping functions f_μ and f_ε in equations (5) and (7), respectively are taken from Abe et al (1992) as:

$$f_\mu = \left\{ 1 - \exp \left[- \frac{(v\varepsilon)^{0.25} n}{14\nu} \right] \right\}^2 \left\{ 1 + \frac{5}{(k^2/v\varepsilon)^{0.75}} \exp \left[- \left(\frac{k^2/v\varepsilon}{200} \right)^2 \right] \right\}, \quad (13)$$

$$f_\varepsilon = \left\{ 1 - \exp \left[- \frac{(v\varepsilon)^{0.25} n}{3.1\nu} \right] \right\}^2 \left\{ 1 - 0.3 \exp \left[- \left(\frac{k^2/v\varepsilon}{6.5} \right)^2 \right] \right\}, \quad (14)$$

where, n is the distance from the nearest wall and ν is the kinematic viscosity. The constants (Equations (6) and (7)) used read, $\sigma_k = 1.4$, $\sigma_\varepsilon = 1.3$, $c_{1\varepsilon} = 1.5$ and $c_{2\varepsilon} = 1.9$.

3. Numerical Method and Results

Flow over the back-step of Figure 1, with and without the porous obstruction, was computed using the control-volume method applied to a boundary-fitted coordinate system with a collocated grid. A hybrid scheme, Upwind Differencing Scheme (UDS) and Central Differencing Scheme (CDS), is used for interpolating the convection fluxes. The SIMPLE algorithm was used to relax the algebraic equations. Low Reynolds damping functions are employed for handling wall proximity. Results were obtained considering an inlet Reynolds number of $Re = 132000$ based on the height of the step H . Inlet conditions for U , k and ε , were used according to values proposed by Heyerichs and Pollard (1996). All boundary conditions are illustrated in Figure 1. The non-linear model employed was the Shih et al (1993) closure. Based on the grid independent study, an orthogonal mesh of size 227×100 was used for the numerical calculations. The solution was considered to be converged when the residual of the algebraic equations is less than a prescribed value of 10^{-5} . Preliminary results for unobstructed flow past a back-step were obtained in order to assess the performance of the linear and non-linear turbulence models in clear domains. Numerical parameters for these cases were $a = 0$, $c_f = 0$, $\phi = 1$ and $K \rightarrow \infty$. The working fluid is air ($\rho = 1.25 [kg/m^3]$, $\mu = 1.8 \times 10^{-5} [Ns/m^2]$, $Pr = 0.72$, $c_{pf} = 1006.0 [J/Kg^\circ C]$) with a uniform inlet temperature of $T = 50^\circ C$. The boundary conditions for the thermal field are constant heat flux ($q_w = 2000.0 [W/m^2]$) on the bottom wall, not including the step, and $q_w = 0$ on the other surfaces. The constant value for the turbulent Prandtl number was $Pr_t = 0.9$.

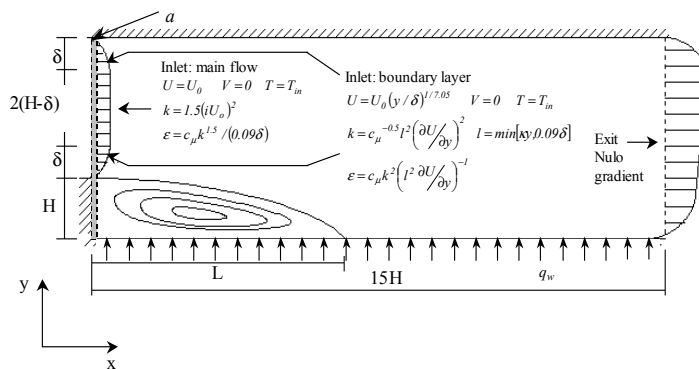


Figure 1: Boundary conditions for turbulent flow past a backward facing step with porous obstruction.

In the following figures, the effect of porosity, thickness and permeability of porous obstruction on the flow pattern will be shown, for turbulent flow, using both the linear and non-linear models with the Low Reynolds Number approach, designated here by **L_LRN** and **NL_LRN**, respectively. In each figure the streamlines are analyzed with the porous material for the following thickness: $a = 0.15H$, $a = 0.30H$ and $a = 0.45H$, where H is the step height. Figure 2 shows also the streamlines considering the channel without the porous obstruction. Figures below show comparisons of streamlines between the linear and non linear closures considering the following permeability and porosity: Fig. 2) $K = 10^6 m^2$, $\phi = 0.85$; Fig. 3) $K = 10^7 m^2$, $\phi = 0.85$; Fig. 4) $K = 10^6 m^2$, $\phi = 0.95$ and Fig. 5) $K = 10^7 m^2$, $\phi = 0.95$.

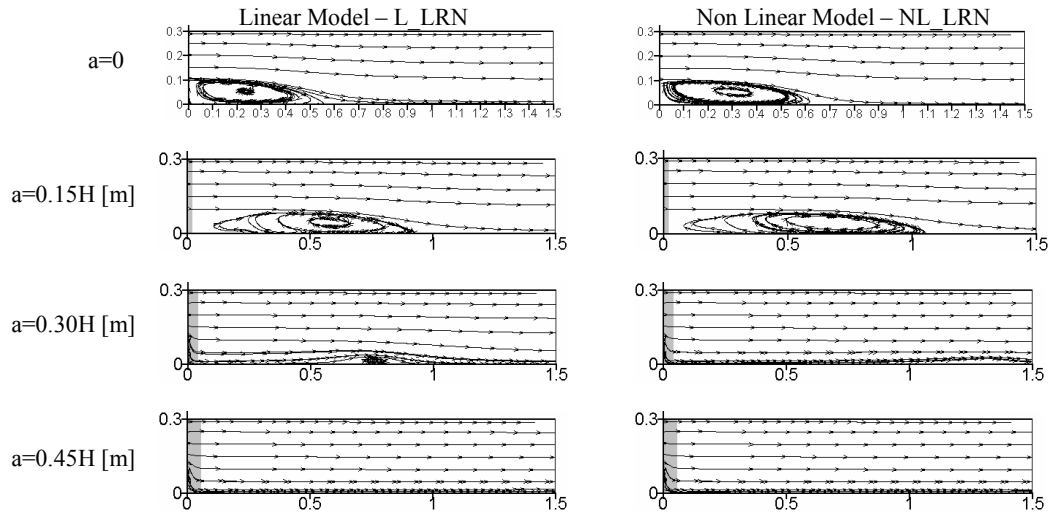


Figure 2: Comparison of streamlines between the linear and non linear models for back step flow with porous obstruction ($K=10^{-6} m^2$, $\phi = 0.85$).

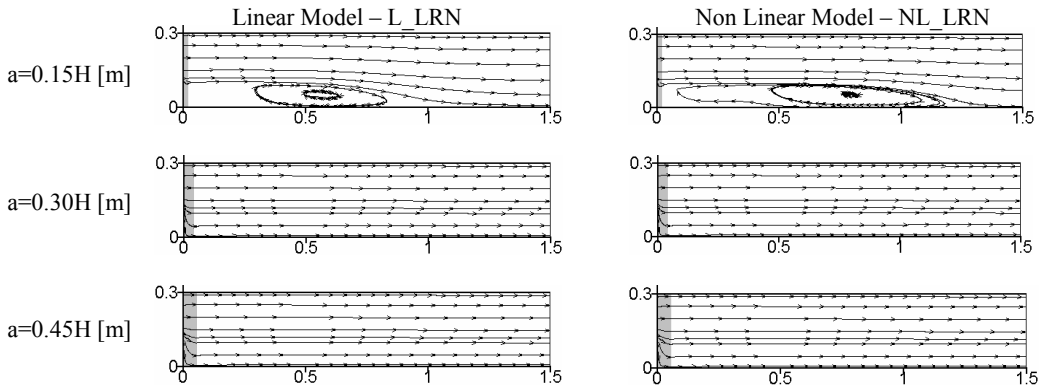


Figure 3: Comparison of streamlines between the linear and non linear models for back step flow with porous obstruction ($K=10^{-7} m^2$, $\phi = 0.85$).

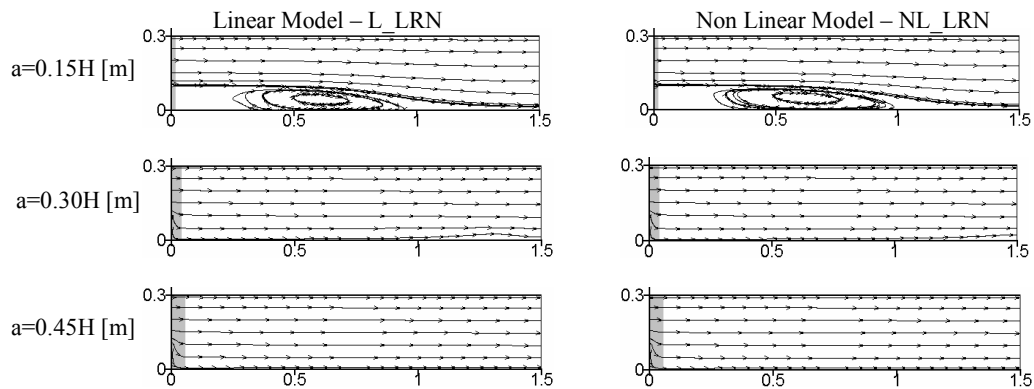


Figure 4: Comparison of streamlines between the linear and non linear models for back step flow with porous obstruction ($K=10^{-6} m^2$, $\phi = 0.95$).

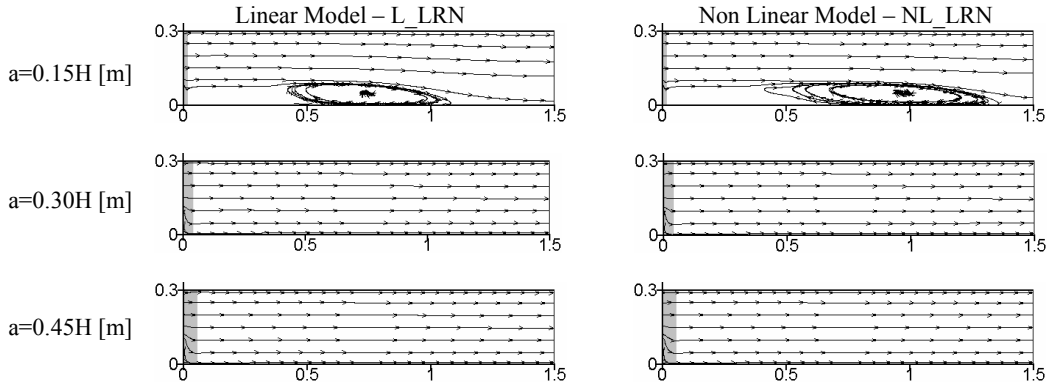


Figure 5: Comparison of streamlines between the linear and non linear models for back step flow with porous obstruction ($K=10^7 \text{ m}^2$, $\phi=0.95$).

It can be noted that the size of the recirculation bubble simulated by the linear model, in cases where $a=0.15H$, is much shorter than the one calculated by non-linear theories. As the thickness of obstruction is increased, the recirculation bubble decreases, and for $a=0.45H$, the recirculation bubble is suppressed, independently of the turbulence model used and values of the permeability and porosity investigated. It is observed that for $K=10^7 \text{ m}^2$, already with $a=0.30H$, the recirculation bubble also is suppressed. From the figures one can further observe that the permeability K and the porosity ϕ of the porous obstruction also plays a role in determining the flow pattern, however their influence on the flow distribution past the obstacle seems to be not as intense as the effect of the thickness a . Or say, by just increasing the value of a one can smooth the flow past the expansion, damping any existing recirculating stream.

Figures 6-9 show distributions for the friction coefficient, C_f and for the Stanton number, St , along the bottom heated wall. These coefficients are given by:

$$C_f = \frac{\tau_w}{\rho U_0^2 / 2}, \quad St = \frac{q_w}{\rho c_{pf} U_0 (T_w - T_{in})} \quad (15)$$

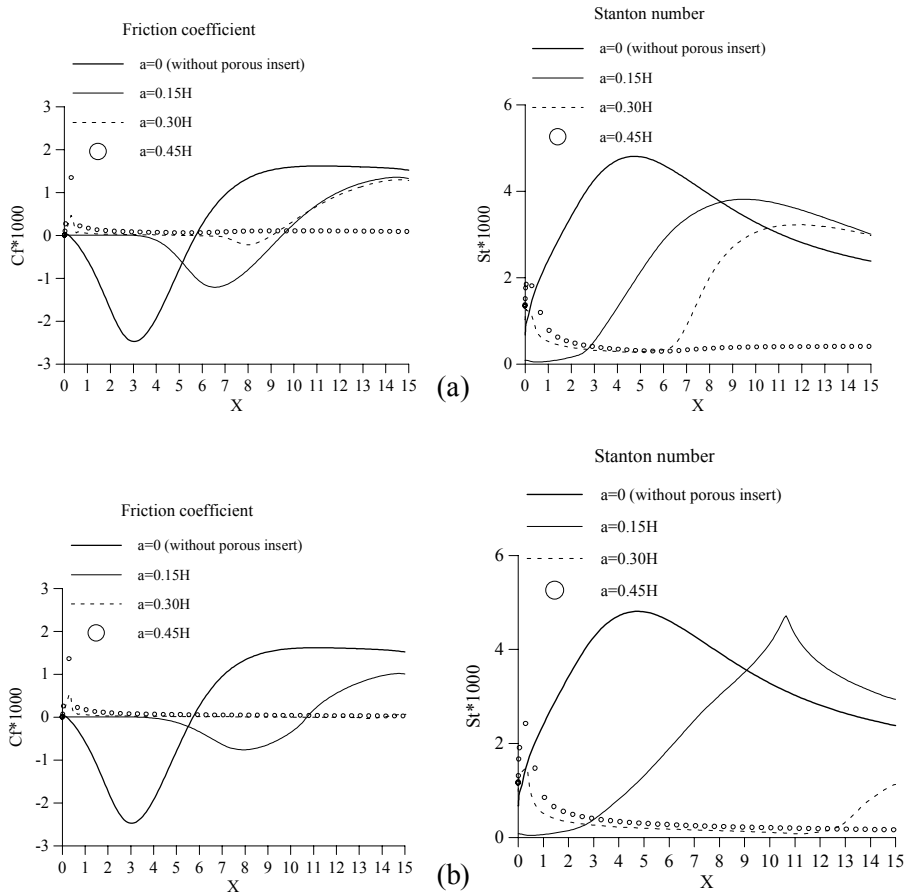


Figure 6: Friction coefficient and Stanton number distribution for $\phi=0.85$ $K=10^{-6} [\text{m}^2]$. (a) L_LRN; (b) NL_LRN.

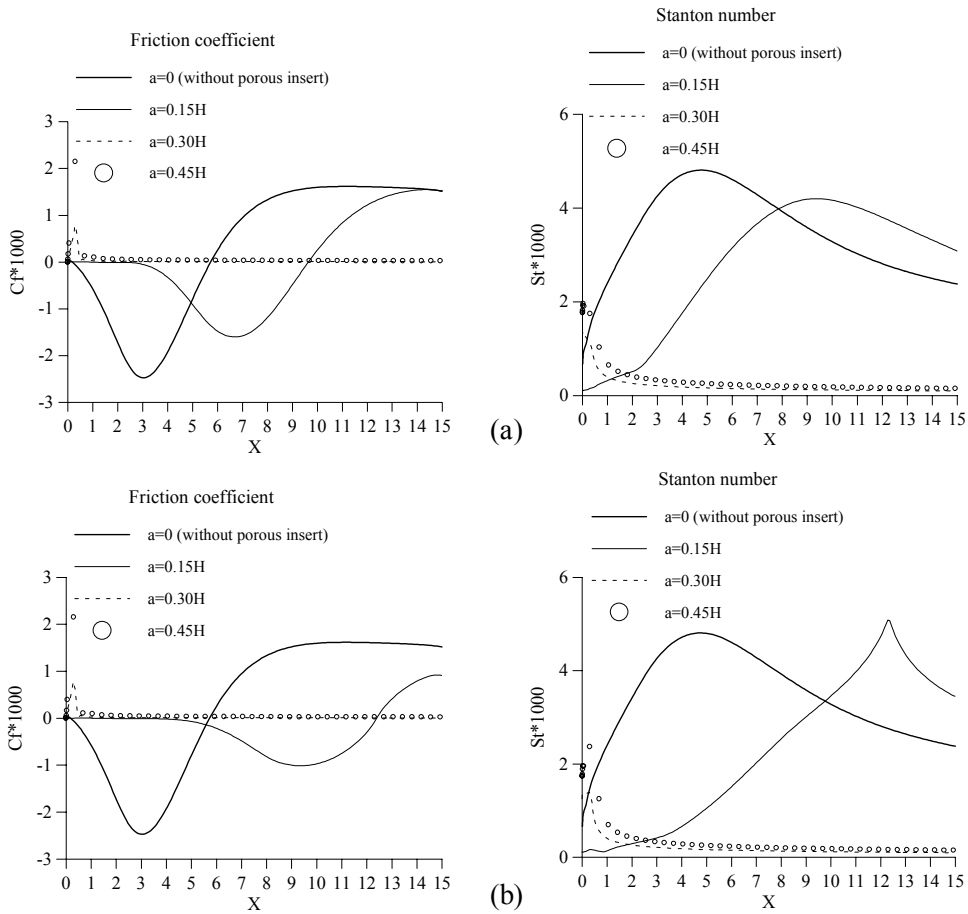


Figure 7: Friction coefficient and Stanton number distribution for $\phi=0.85$ $K=10^{-7}$ [m^2]. (a) L_LRN; (b) NL_LRN.

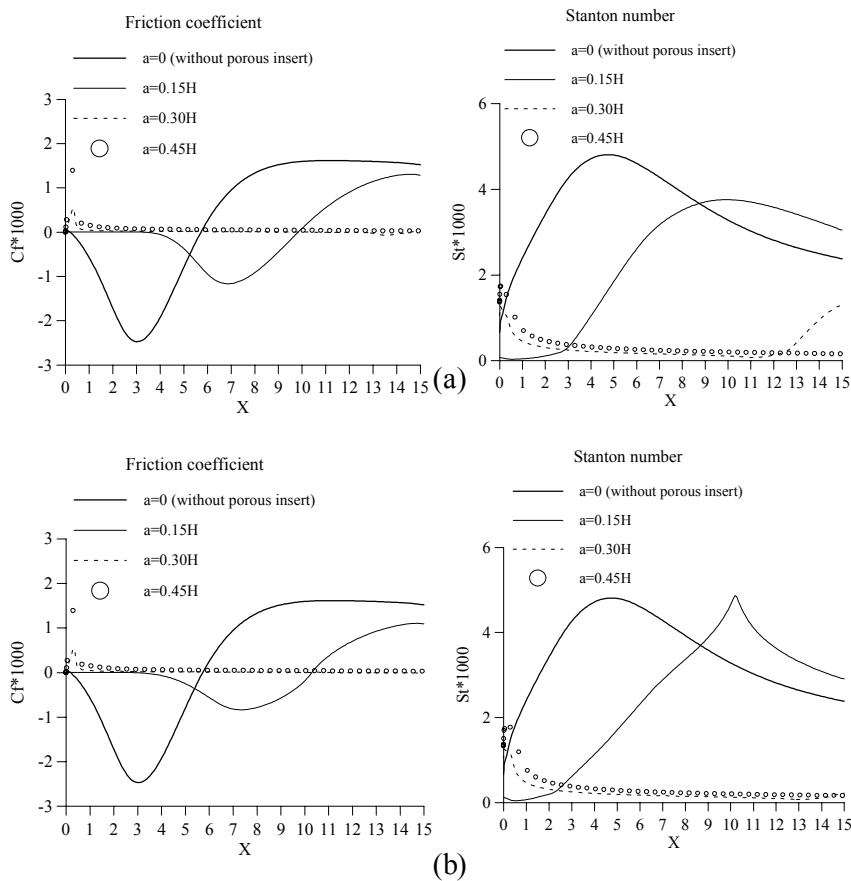


Figure 8: Friction coefficient and Stanton number distribution for $\phi=0.95$ $K=10^{-6}$ [m^2]. (a) L_LRN; (b) NL_LRN.

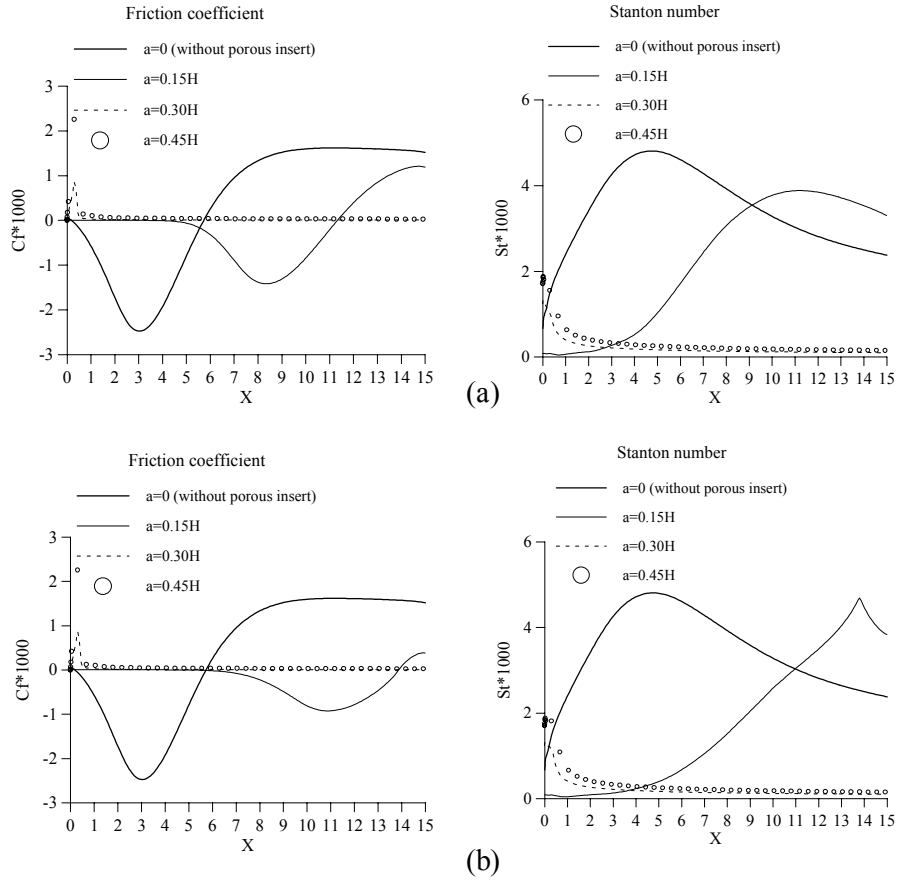


Figure 9: Friction coefficient and Stanton number distribution for $\phi=0.95$ $K=10^{-7}$ [m^2]. (a) L_LRN; (b) NL_LRN.

Again one should note the expressive effect of the thickness on the porous obstruction on the calculated parameters. The distributions for both the Stanton number and the friction coefficient follow the same path in regard to the sensitivity of the type of model used. Or say, as the thickness of the obstruction increases, both linear and non-linear models predict comparable results since the size of the recirculating bubble decreases. It is interesting to emphasize that for $a=0.45H$ profiles for St are flattened, a feature that can be used to great advantage when optimizing engineering flows. The sudden increase of St around the reattachment point, known to be undesirable in many practical situations for causing additional thermo-mechanical loads on the surface material, may be avoided by the use of a porous plate. Overall, one can say that the thickness of the obstruction plays the dominant role in changing the final flow pattern rather than the porosity or permeability of the material.

Figure 10 shows the normalized turbulent kinetic energy distributions for both the linear and non-linear models. It shows the turbulent kinetic energy field considering a clean channel and also the channel with a porous insert for a permeability of $K=10^{-6}$ m^2 and porosity of $\phi=0.85$. The thicknesses of $a=0.15H$ and $a=0.45H$ are used. The values of non-dimensional turbulent kinetic energy obtained are in the form:

$$KN = \frac{k - k_{\min}}{k_{\max} - k_{\min}}, \quad (16)$$

where k_{\min} and k_{\max} represent the maximum and minimum values, respectively, in the computational domain.

The turbulence models present different results for the clean channel with an accentuated distribution of k , however, for the channel with a porous insert the models produce the same results and it is observed that the high k values occur in the entrance of the geometry, more specifically they concentrate all in the porous obstacle.

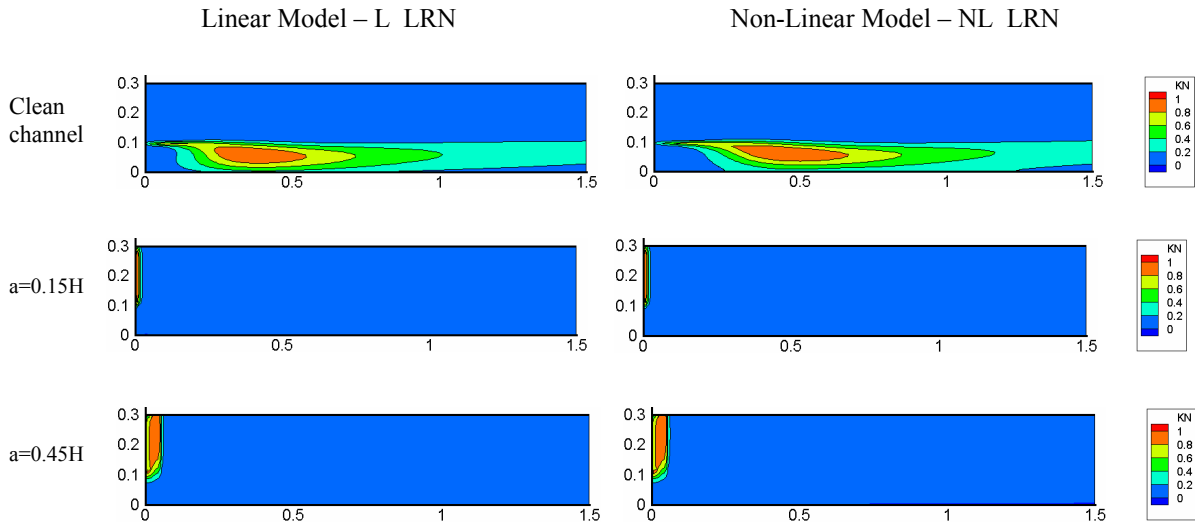


Figure 10: Turbulent kinetic energy fields for turbulent flow past a backward-facing-step channel with a porous obstruction with $K=10^{-6} m^2$ and $\phi = 0.85$.

4. Conclusions

In this work, two turbulence models (linear and non-linear), using low Reynolds number functions, have been used to simulate convective heat transfer in a flow past a backward-facing step with a porous obstruction. Parameters such as porosity ϕ , permeability K , and thickness a of the porous material were varied in order to analyze their effects on the flow pattern and thermal field.

For validation, results without the obstruction were compared with experimental data of Kim *et al.* (1980). The experimental value for the separation length given in the literature is $x_R / H = 7.0$. The linear and non-linear models resulted in $x_R / H = 5.65$ and $x_R / H = 6.55$, respectively, indicating an advantage of non-linear closures in predicting more realistic results.

Figures 2-5 showed that the recirculating bubble simulated with the linear model was always shorter than the one calculated with non-linear theories. Also, results of friction coefficient (C_f) and Stanton number (St) distribution indicate that the thickness of the obstruction had a more pronounced effect in suppressing the recirculation bubble than other parameters such as the permeability or the porosity. It has also been observed that the total damping of the recirculation bubble occurred for $a=0.45H$, independently of the turbulence model employed and for $K = 10^{-7} m^2$ with a thickness of $a=0.30H$, the recirculation bubble also is suppressed.

It is known that the placement of a porous material inside a fluid passageway produces resistance to the flow, which results in the form of a pressure loss in the downstream locations. This is the penalty that has to be overcome by an increased pumping power to maintain the flow, however the attenuation or even the suppression of the recirculating bubble decreases the risk of an overheating on the surface, more specifically around the reattachment point. Those findings may be used to advantage by design engineers when optimizing thermo-mechanical equipment.

5. Acknowledgement

The authors would like to thank FAPESP and CNPq, Brazil, by their financial support during the obtaining of these results.

6. References

- Abe, K., Nagano, Y., Kondoh, T., 1992, "An improved $k-\epsilon$ model for prediction of turbulent flows with separation and reattachment", *Trans. JSME, Ser. B*, vol. 58, pp. 3003-3010.
- Assato, M., de Lemos, M.J.S., 2000, "Secondary Flow in Ducts of Non-Circular Cross Section Using a Non-linear k- ϵ Model", *Proc. of ENCIT2000 - 8th. Braz. Congr. of Thermal Eng. and Sciences* (on CD-ROM), Porto Alegre, RS, Brazil, October 3-6 (In Portuguese).
- Assato, M., Pedras, M.H.J. & de Lemos, M.J.S., 2002, "Numerical Solution of Turbulent Flow Past a Backward-Facing-Step With a Porous Insert Using Linear and Non-Linear k- ϵ Models", *Proc. of APM2002 - 1st Inter. Conf. on Applications of Porous Media*, Paper APM-163, V. CDROM, Eds. R. Bennacer and A.A. Mohamed, 2002. v.1. p.539 – 550, June 2-8, Jerba, Tunisia.

- Beavers, G.S and Joseph, D.D., 1967, *J. Fluid Mechanics*, vol. 30, 197.
- Brinkman, H.C., 1948, "Calculations of the Flow of Heterogeneous Mixture Through Porous Media" *Applied Science Research*, 2, pp. 81-86.
- Chan, E.C., Lien, F.S. and Yovanovich, M.M., 2000, "Macroscopic Numerical Study of Forced Convective Heat Transfer in a Back-step Channel Through Porous Layer", *Proceedings of NTHC2000, ASME National Heat Transfer Conference*, 20th–22th August, 2000, Pittsburgh, Pennsylvania, USA.
- de Lemos, M.J.S., Sesonske, A., 1985, "Turbulence Modeling In Combined Convection In Liquid-Metal Pipe Flow", *Int. J. Heat & Mass Transfer*, vol. 28, #6, pp. 1067-1088.
- de Lemos, M.J.S., 1988, "Anisotropic Turbulent Transport Modeling For Rod-Bundle", *Int. J. of Heat & Technology*, vol. 6, # 1-2, pp. 27-37.
- Heyerichs, K., Pollard, A., 1996, "Heat Transfer in Separated and Impinging Turbulent Flows", *Int. J. Heat Mass Transfer*, Vol. 39, n^o 12, pp. 2385-2400.
- Jones, W.P. and Launder, B.E., 1972, "The Prediction of Laminarization with Two-Equation Model of Turbulence ", *Int. J. Heat & Mass Transfer*, Vol. 15, pp. 301 - 314.
- Kim, J., Kline, S.J., Johnston, J.P., 1980, "Investigation of a Reattaching Turbulent Shear Layer: Flow over a Backward-Facing Step", *ASME J.Fluids Engng*, 102, pp. 302-308
- Lumley, J.L., 1970, " Toward a Turbulent Constitutive Relation", *J. Fluid Mech.*, 41, 413.
- Nield, D.A. and Bejan, A., 1992, "Convective in Porous Media" , Springer-Verlag.
- Nisizima, S. and Yoshizawa, A., 1987, "Turbulent Channel and Couette Flows Using an Anisotropic $k-\varepsilon$ Model", *AIAA J.*, Vol. 25, N^o 3, p. 414.
- Ochoa-Tapia, J. A.; Whitaker, S., 1995, "Momentum Transfer at the Boundary between a Porous Medium and a Homogeneous Fluid-I. Theoretical Development.", *Int. J. Heat Mass Transfer*, vol. 38, pp. 2635-2646.
- Pedras, M.H.J. and de Lemos, M.J.S., 2001a, "Macroscopic Turbulence Modeling for Incompressible Flow Through Undeformable Porous Media". *Int. J. Heat Mass Transfer*, vol. 44 (6), pp. 1081-1093.
- Pedras, M.H.J. and de Lemos, M.J.S., 2001b, "On Mathematical Description and Simulation of Turbulent Flow in a Porous Medium Formed by an Array of Elliptic Rods". *ASME Journal of Fluids Engineering*, vol. 123 (4), pp. 941-947.
- Pedras, M.H.J. and de Lemos, M.J.S., 2001c, "Simulation of Turbulent Flow in Porous Media Using a Spatially Periodic Array and a Low Re Two-Equation Closure". *Numer. Heat Transfer Part A-Appl*, vol. 39 (1), pp. 35-59.
- Pedras, M.H.J. and de Lemos, M.J.S., 2002, Computation of Turbulent Flow in Porous Media Using a Low Reynolds $k-\varepsilon$ Model and an Infinite Array of Transversally-Displaced Elliptic Rods, *Numer. Heat Transfer Part A-Appl (in press)*.
- Rivlin, R.S., 1957, "The Relation Between the Flow of Non-Newtonian Fluids and Turbulent Newtonian Fluids", *Q. Appl. Maths*, 15, 212.
- Rocamora, Jr, F.D. and de Lemos, M.J.S., 2000, Heat Transfer in Suddenly Expanded Flow in a Channel with Porous Inserts", *Proceedings of NTHC2000, ASME National Heat Transfer Conference*, 20th –22th August, 2000, Pittsburgh, Pennsylvania, USA.
- Rubinstein, R. & Barton, J.M., 1990, "Renormalization Group Analysis of the Stress Transport Equation", *Phys Fluids A* 2, pp. 1472.
- Shih, T.H., Zhu, J. and Lumley, J.L., 1993, "A Realizable Reynolds Stress Algebraic Equation Model", *NASA TM-105993*.
- Speziale, C.G., 1987, "On Nonlinear $k-l$ and $k-\varepsilon$ Models of Turbulence", *J. Fluid Mech.*, vol. 176, pp. 459-475.
- Vafai, K. and Kim, S.J., 1990, *Int. J. Heat and Fluid Flow*, 11, 254.
- Vafai, K., Tien, C. L., 1981, "Boundary and Inertia Effects on Flow and Heat Transfer in Porous Media", *Int. J. Heat Mass Transfer*, vol. 24, pp. 195-203.